Parallel Position/Force Control of Epicardial Wire Robot Based on Ellipsoid Geodesy

E. Wilde[1], S. Dan[2], N. A. Wood[3], M. J. Passineau[4], M. S. Halbreiner[4], M. A. Zenati[5], and C. N. Riviere[6]

***Abstract*— Gene therapies are emerging as an increasingly promising treatment for congestive heart failure. However, their effectiveness is linked to the method for delivery to the target region of the heart. Current methods lack an approach for minimally invasive, uniform delivery. To address this need we developed Cerberus, a minimally invasive parallel wire robot for cardiac interventions. Accurate and safe interventions using this device require regulation of force in addition to injector position. Prior work on Cerberus involved developing and implementing a parallel position/force controller for a simplified planar model. This work adapts the Cerberus robot to explore the effectiveness of a control approach that accounts more realistically for the geometry of the heart by modeling it as a prolate ellipsoid.**

I. INTRODUCTION

Heart failure is a serious affliction and a leading cause for mortality in the world. It has been estimated that nearly 23 million people are afflicted with heart failure [1]. While there are certain small-molecule drugs and implantable devices that have been helpful with more common cardiac issues, patients with heart failure still experience health conditions and recurring hospitalizations [1], [2]. However, a growing understanding of myocardial dysfunction and gene transfer technology have led to the promise of effective gene therapy drugs for congestive heart failure [2].

While gene therapies for congestive heart failure show promise, the effectiveness is influenced by the amount of gene transferred to the target tissue, which is dependent on the delivery method [3]. Current methods of gene therapy application to the myocardial tissue lack an effective way to deliver an efficacious dose and a uniform distribution of the drug [3]. These methods include intravascular injections, direct intramyocardial injections, and pericardial injections [4]. Intravascular injection methods include peripheral intravenous injections, antegrade coronary injections, retrograde coronary injection, and aortic clamping. However, disadvantages of intravascular injections for gene therapy can include dilution, limited delivery area, expression in non-targeted areas, and more [4]. To date, direct myocardial injections also have disadvantages due to limited ability to reach the entire target region and limited dexterity [4]. To avoid this issue and adequately conduct direct myocardial injections with existing instrumentation would require invasive surgery, drastically increasing recovery time and risk of infection [5]. Pericardial injections can suffer from gene expression in non-targeted areas due to possible leakage, and ineffective dose delivery due to gene transduction being primarily to the pericardial cells rather than the myocardial cells [4]. Where these methods have drawbacks, robotics has potential to offer solutions that expand the surgical workspace and provide accurate control for uniform delivery while being minimally invasive. If a robotic system is capable of operating on the beating heart, this has potential to also reduce morbidity [6].

The HeartLander robotic system is designed for minimally invasive injections into the beating heart [7]. This system is a miniature mobile robot that crawls on the surface of the beating heart and has proven itself to be a viable option for semiautonomous epicardial injections. However, the system lacks the ability to perform scores or hundreds of injections rapidly over a large workspace, which limits its effectiveness in gene therapy applications in which uniform delivery of the gene drug over a large area (e.g., the free wall of the left ventricle) is of crucial importance.

Cerberus is a parallel wire robot developed to bridge the functional gap left by HeartLander, by conducting minimally invasive cardiac interventions quickly and efficiently over a large workspace [8]. Cerberus is inserted using a subxiphoid approach similar to HeartLander. Cerberus includes three suction bases and a mobile base intended to house a hypodermic needle for cardiac interventions. Two of the suction bases are at the ends of flexible arms and the third is at the base of both arms. Once inserted, the flexible arms expand into a triangular shape and adhere to the surface of the beating heart with suction at the three vertices. Wires from each base connect to an injector head that moves within the triangular support structure by changing the wire lengths. Figure 1 represents a model for Cerberus where the flexible arms have extended to their maximum distance from the middle vertex or point of entry , giving an operating region over an elliptical surface. This parallel wire design allows for quick movement over the region within the triangular region delimited by the manipulator [9]. This design also shares the benefits of organ-mounted robots, namely a stable platform with approximately zero motion relative to the heart [10].

Previous work on Cerberus focused on adapting previously

Funding provided by National Institutes of Health (grant no. R01HL078839).

[1] E. Wilde is with the Electrical and Computer Engineering Department, Carnegie Mellon University, Pittsburgh, PA 15213.

[2] S. Dan is with the Mechanical Engineering Department, Carnegie Mellon University, Pittsburgh, PA 15213.

[3] N. A. Wood is with Virtual Incision Corp., Sioux Falls, SD 57108.

[4] M. J. Passineau and M. S. Halbreiner are with Allegheny General Hospital, Pittsburgh, PA 15212.

[5] M. A. Zenati is with Harvard Medical School, Boston, MA 02115.

[6] C. N. Riviere is with the Robotics Institute, Carnegie Mellon University, Pittsburgh, PA 15213 USA (e-mail: camr@ri.cmu.edu).

978-1-5386-7825-1/19/$31.00 ©2019 IEEE

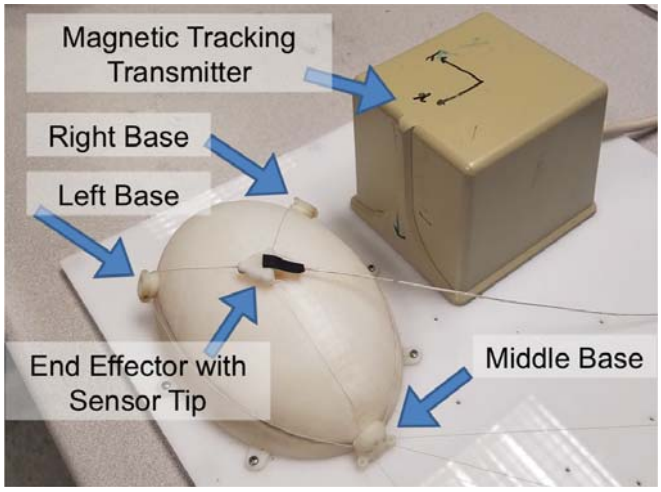

Fig. 1. Benchtop mock-up of Cerberus for control system development on a prolate ellipsoid. The magnetic tracking system tracks a 6-degree-of-freedom sensor implanted in the end-effector for localization.

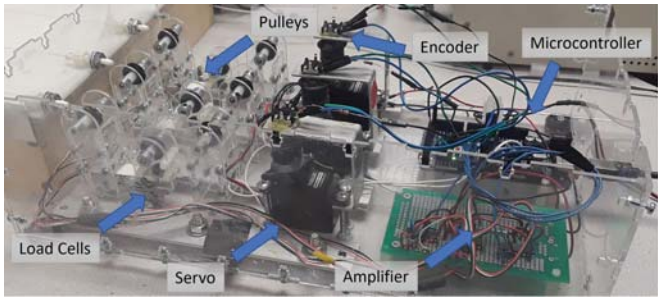

Fig. 2. Primary control hardware includes the Arduino Mega 2560, continuous-rotation servos, rotary encoders, and load cells.

developed methods for parallel cable manipulators to the system [11], [12]. These previous models generally used simplifying assumptions about the geometry of the robot and were designed for planar systems. Therefore, the inverse kinematics to determine the wire lengths and the statics model and methodology to derive optimal tensions in previous work also operated under a planar assumption [8]. The present work has adapted Cerberus to operate on the curved surface of a prolate ellipsoid to better represent the curvature of the heart. In this paper, we present a system that demonstrates this capability by implementing geodetic inverse kinematics with appropriate three-dimensional statics to develop a parallel position/force control system for Cerberus.

II. Methods

A. System Hardware

The Cerberus system incorporates a combination of pulleys and load cells to measure the tension in each wire [8]. The wires are made of braided ultra-high-molecular-weight polyethylene. The system adheres to the epicardium using suction [13], but the present study used a benchtop mockup of the device designed for evaluation of control approaches,

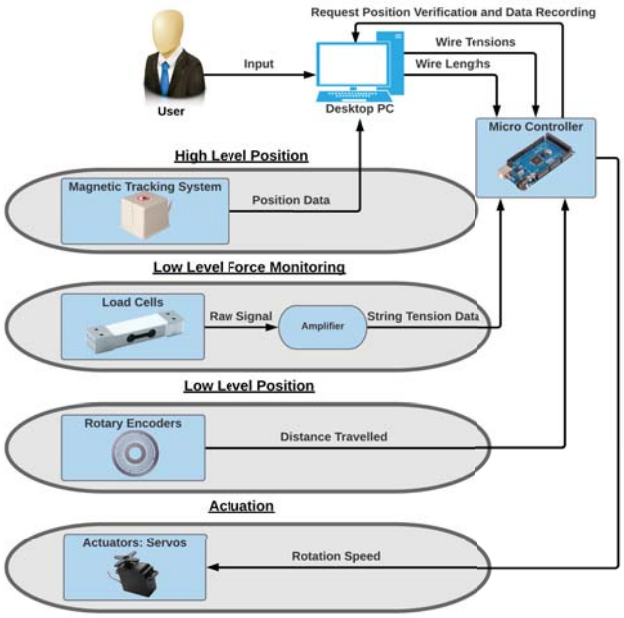

Fig. 3. System diagram describing data flow between hardware components in the robotic system. System diagram also indicates primary function associated with hardware components.

in which the three bases are firmly affixed to the surface of a prolate ellipsoid (Figure 1). The control hardware, designed to remain external to the body, can be seen in Figure 2. A microBIRD electromagnetic tracker (Ascension Technologies) is mounted within the injector head, with the magnetic field source set a short distance away. Calibration of the electromagnetic tracking system relative to the origin of the ellipsoid and subsequent tracking of the sensor gives position information that is used for end-effector localization, inverse kinematics solutions, and statics solutions.

B. System Overview

The Cerberus system shown in Figure 3 incorporates a primary control computer which takes input from the user in the form of desired end-effector positions on an ellipsoid model. The electromagnetic tracker system is used to identify three-dimensional Cartesian coordinates of the injector head resting on the surface of an ellipsoid heart model. This tracker system is integrated with Matlab and the primary Cerberus GUI. Desired wire tensions and the calculated difference of the wire lengths are then transmitted from the primary computer to the micro-controller. Within the control box are a set one for each wire of rotary encoders, load cells, and continuous rotation servos attached to fixed-diameter spools wrapped in wire. The rotary encoders are used to estimate the amount of cable released or retrieved and subsequently the movement of the end-effector. Load cells, amplifiers, and a pulley system are used to measure tension in each of the wires. Both the encoder values and measured tension from the load cells are used by the micro-controller for low-level control of position and force. Finally,

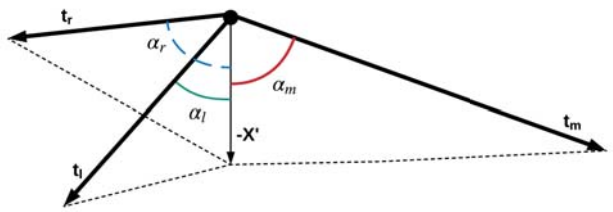

Fig. 4. Free body diagram of end-effector on the model prolate ellipsoid in 3D. Tensions in each cable define the force vectors applied to the end-effector. Angles designated by between the applied tension vectors and the end-effector normal vector designated by X0 are used in system force balance equations.

the micro-controller intermittently sends requests to the main control computer to verify global position and record data.

C. Inverse Kinematics

Prior implementations of the inverse kinematic equations focused on determining the distances between the end-effector and the bases in a planar model where these distances were found by drawing concentric circles around each base that intersect at the injector to find the Euclidean distance between each base assuming that the middle base is set as the origin under Cartesian coordinates [8]. With a three-dimensional ellipsoid model, the approach to determining the cable lengths (distances) between end-effector and bases is focused on calculating geodesics, the shortest distances between two points on a curved surface. After defining the ellipsoid models radii, eccentricity, and flattening coefficients, solutions are found using a inverse geodesics approach involving a root finding method with Newtons method [14].

D. Statics

A three dimensional free body diagram of the system can be seen in Figure 4. A coordinate frame local to the end-effector is used when formulating system equations. The resulting statics equations are given by:

$$\Sigma F_x = t_l cos\alpha_l + t_m cos\alpha_m + t_r cos\alpha_r \tag{1}$$

$$\Sigma F_y = t_l cos\phi_l + t_m cos\phi_m + t_r cos\phi_r \tag{2}$$

$$\Sigma F_z = t_l sin\phi_l + t_m sin\phi_m + t_r sin\phi_r \tag{3}$$

where t_l, t_m, and t_r are tensions applied to the left, middle, and right wires, respectively. The above set of equations can also be viewed as:

$$ST = F \tag{4}$$

$$S = \begin{pmatrix} cos\alpha_l & cos\alpha_m & cos\alpha_r \\ cos\phi_l & cos\phi_m & cos\phi_r \\ sin\phi_l & sin\phi_m & sin\phi_r \end{pmatrix}, T = \begin{pmatrix} t_l \\ t_m \\ t_r \end{pmatrix}, F = \begin{pmatrix} F_n d \\ 0 \\ 0 \end{pmatrix} \tag{5}$$

After defining F_{nd} as the desired normal force that the end-effector should apply to the ellipsoid surface and then solving for the tensions, a unique solution can be found for any reachable position on the ellipsoid surface. The remainder of this section is denoted to determining the α and φ values in the system force balance equations. The angles designated by α refer to the angles between the respective tension vector and the normal vector into the surface of the ellipsoid at the end-effector location. These angles are in the plane made by the respective tension vector and the aforementioned normal vector. These α values are found by first identifying the normal vector to the ellipsoid surface at the end-effector location. The ellipsoid can be represented by:

$$\frac{x^2}{a^2} + \frac{y^2}{b^2} + \frac{z^2}{c^2} = 1 \tag{6}$$

For the prolate ellipsoid, a and b both equal the equatorial radius R, and c equals the pole radius R_p. Given the global Cartesian coordinates (x,y,z) of the end effector relative to the origin of the ellipsoid, the normal vector can be found by taking the gradient of the ellipsoid at the point.

$$\Delta f(x,y,z) = (\frac{2\hat{x}}{R^2}, \frac{2\hat{y}}{R^2}, \frac{2\hat{z}}{R_p^2}) \tag{7}$$

After calculating the normal vector, the appropriate tension vectors need to be calculated. Each tension vector is first approximated by taking differences between end-effector location and base location while ignoring the ellipsoid surface. However, in the physical system the wires are affected by ellipsoid geometry. The attachment points of the wires to the end-effector are a small distance above the surface of the ellipsoid, and the wires will possess a linear portion between the attachment point on the end-effector and the initial tangent contact point on the ellipsoid surface. Evaluating the linear portion of the wire can lead to determining the α values. To better approximate the tension vectors (linear portion of the wire) affected by the ellipsoid geometry, the initial contact points of the wires on the ellipsoid need to be found. This is found by running an optimization algorithm with the following constraints:

$$A_0 x + B_0 y + C_0 z + D = 0 \tag{8}$$

$$\frac{2x}{R^2} + \frac{2y}{R^2} + \frac{2z}{R_p^2} - 1 = 0 \tag{9}$$

$$(-R, -R, -R_p) < (x, y, z) < (R, R, R_p) \tag{10}$$

$$\hat{n} \cdot \hat{v} = 0 \tag{11}$$

Equation (7) refers to the plane encompassing both the normal vector and one of the approximate tension vectors v_b that ignores the geometry of the ellipsoid. It is assumed for this portion of the analysis, that the contact point of the wire lies in line with the vector v_b. Equation (8) indicates the upper and lower bounds for the contact point to be found. Equation (9) is a constraint indicating that the normal to the ellipse at the solution point should be orthogonal to the tension vector found using the solution point and attachment point at the end-effector location. The optimization algorithm *fmincon* in Matlab will give the initial tangent contact point

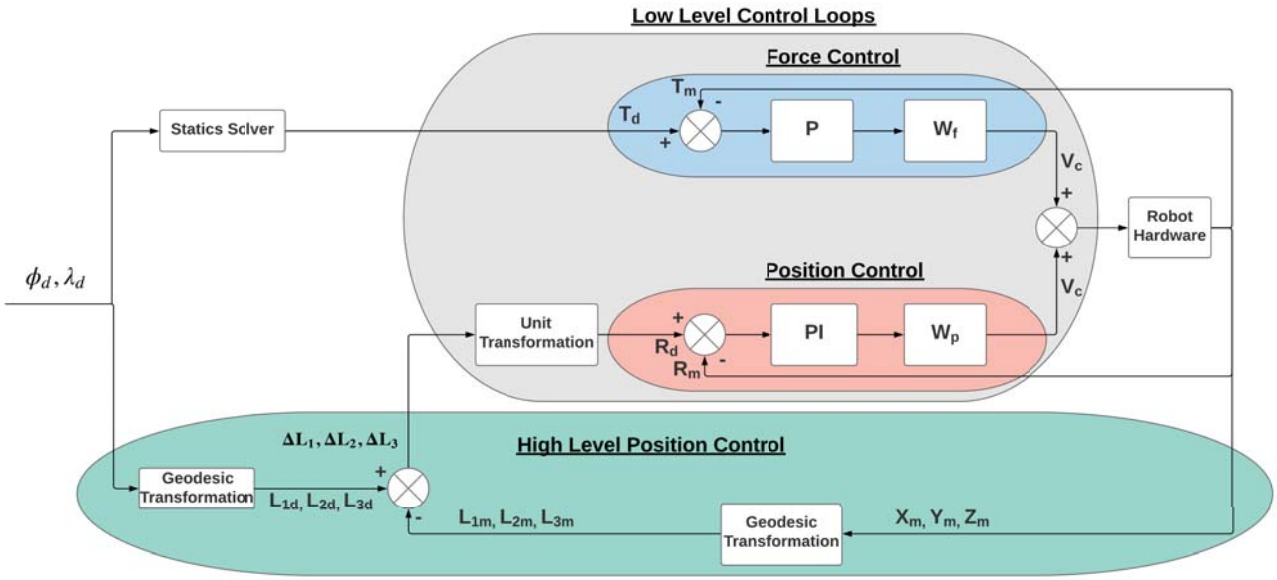

Fig. 5. Parallel control structure implemented in the Cerberus robotic system. The statics solution and high-level position control are run on the primary desktop PC while low-level control is run on the microcontroller.

for each wire, from which the more accurate tension vector can be derived. The α -values can then be found using:

$$\alpha = acos \frac{\bar{t} \cdot -\overline{X^l}}{||\bar{t}|| \cdot ||\overline{-X^l}||} \tag{12}$$

In this equation, *t* refers to a tension vector and *-X'* refers to an end-effector local coordinate axis, which aligns with the normal into the ellipsoid at the end-effector location. Determining φ_l, φ_m, and φ_r, can be done after first projecting the three tension vectors onto the plane that is orthogonal to the normal of the ellipsoid at the end-effector location. The projection of the 3 dimensional tension vectors onto the plane can be done by subtracting components of the vector that are orthogonal to the plane as shown in Equation (13).

$$proj_{Plane}(\bar{t}) = \bar{t} - \frac{\overline{t_p} \cdot \overline{p}}{||\overline{p}||^2}\overline{p} \tag{13}$$

In this equation, *t* refers to a tension vector and refers to the plane normal. The projected vectors are referred to as t_{lp}, t_{mp}, and t_{rp}. The angles φ_l, φ_m, and φ_r can all be found by evaluating equation (14). φ_m is always set to 180deg and aligned with the Z axis as a simplifying assumption.

$$\phi = acos \frac{\overline{t_p} \cdot -\overline{Z^l}}{||\overline{t_p}|| \cdot ||\overline{-Z^l}||} \tag{14}$$

In this equation, t_p refers to a projected tension vector and *Z* refers to an end-effector local coordinate axis.

E. Parallel Position/Force Control

The Cerberus control system incorporates a Parallel position/force control model that combines 3 control variables with 2 levels of hierarchical control loops. The electromagnetic tracker system is used to identify three-dimensional Cartesian coordinates of the injector head resting on the surface of an ellipsoid heart model. This information is then transformed into ellipsoidal coordinates of latitude and longitude signified by φand λ. Given the position of the injector head and relative location of the mounting bases, the distances between the injector head and the bases are calculated with inverse kinematics of prolate ellipsoids in Matlab. These distances are also viewed as the wire-lengths between each base and the injector head. Given a desired position input, the difference between each of the wire lengths for the current position and desired position of the injector head is calculated as the change of wire lengths. The statics model solves for the desired tension values for each wire for a given end-effector position to create a statically stable system. The wire tensions and the calculated difference of the wire lengths are then transmitted over serial from the primary computer to the microcontroller. The microcontroller runs a parallel position/force control model on the tensions in the wires and wire lengths, respectively. Both the position and force control loops use PI controllers to operate. Additional weights for force and position signified by W_f and W_p, respectively. in Figure 5, are used to control the relative effect of each control loop on the final output. Once the low-level position and force controllers have allowed their respective control variables to reach the setpoint values, a request is sent to the high-level position controller to verify the recorded position and send values for adjustment if necessary.

III. Results

Experiments run on the Cerberus platform compared varying levels of force control with values of 0%, 20%, and 40% in respect to the total levels of position control. The results from the 40% case are shown in Figure 6. The Matlab

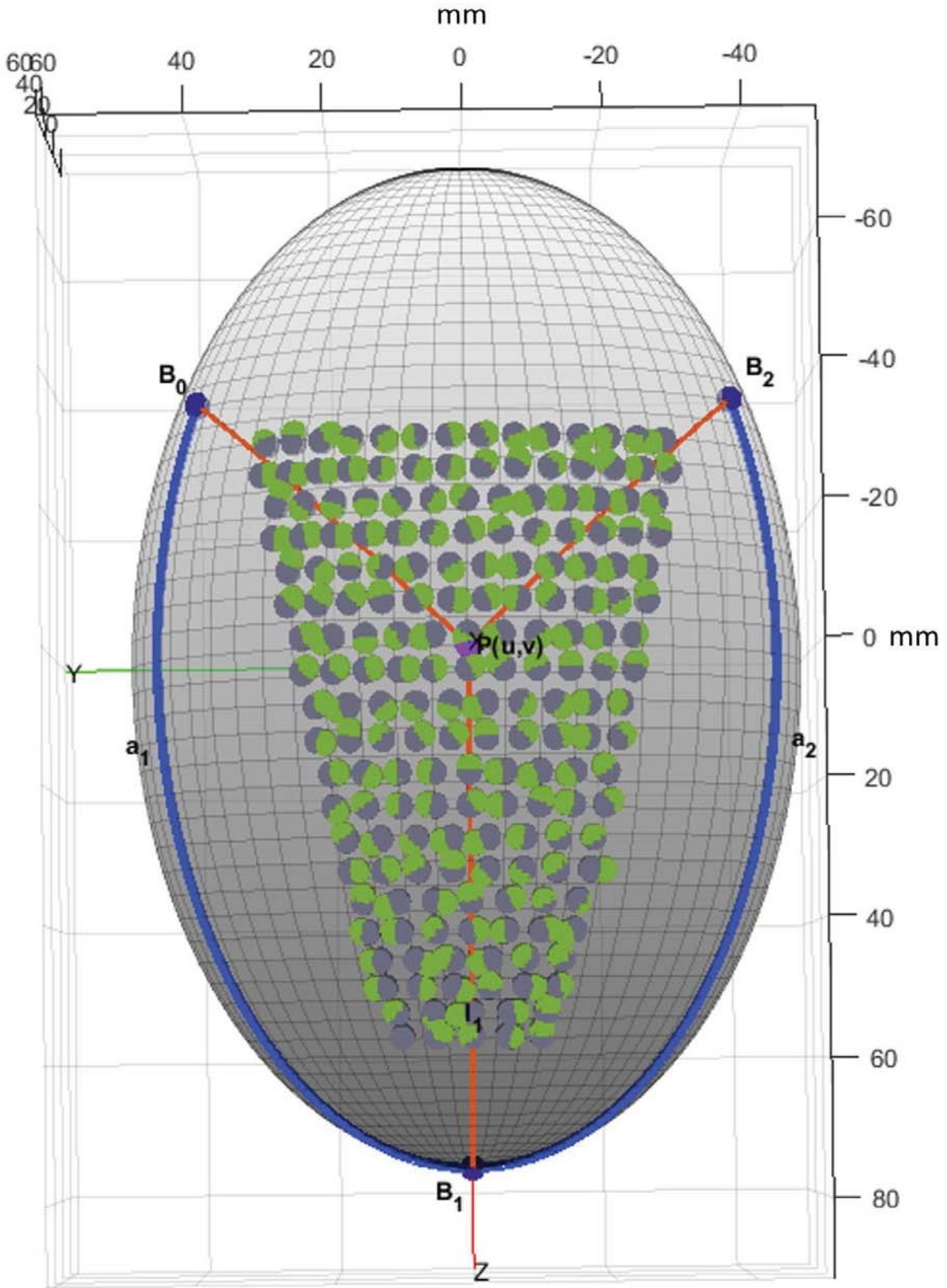

Fig. 6. Sagittal view of representative elliptical operating surface with experiment results. Gray points indicate target points and green points indicates recorded points. B_0, B_1, B_2 represent the 3 bases adhered to the surface of the ellipse. The red lines, a_1, and a_2 represent wire lengths. The purple point represents the current recorded point of the end effector by the electromagnetic tracking system. All 190 points displayed have a radius of 2mm

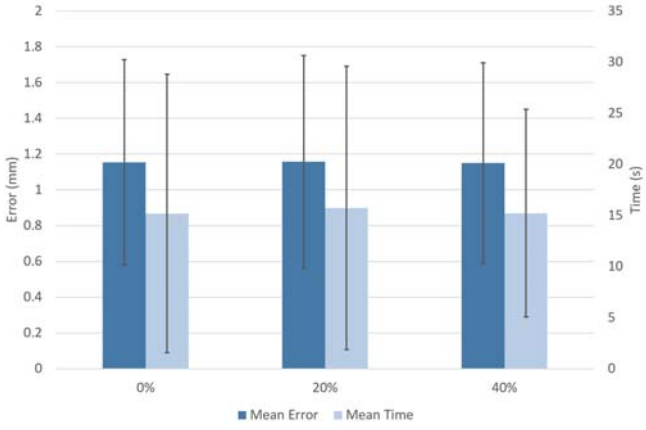

Fig. 7. Data collected across various test iterations for the range of weights for force control from 0%, 20% and 40% of the positional control on a triangular grid with 5mm spacing and 1140 points

code incorporates an additional 1-second time delay with each adjustment required to move to each desired point. For each desired end-effector location, the mean and standard deviation of time between points and the distance error relative to the desired position are calculated and can be seen in Figure 7. All test runs are completed with wire length tolerances of 1mm in regard to the recorded position of the end effector by the tracking system.

Position control alone can yield system states where the end effector would take a significant amount of time to converge upon the desired point and tension values, which would either run largely beyond expected tolerable values or run below the necessary value impacting the end-effector's orientation and effective normal force in relation to the ellipsoid. Despite the 1140 test points collected for 0% force control being shown in Figure 7, the system at force control weights below 20% has been found to fail at times due to either excessive tension or a lack of tension in the wires.

IV. Discussion

It is clear that position-only control is not a viable solution when operating the Cerberus model on prolate ellipsoids, as shown by the control failures just mentioned above. As position-only control only takes in changes in wire-lengths, the system has no method of evaluating or regulating wire tensions, and the system would need precise setup for the initial starting position. The low-force-control cases are unable to compensate for the desired tension values for the statics model which becomes a significant factor for points lying close to the limits of the range of motion. The parallel position/force controller at ratios above 20% does a more adequate job of reaching desired end-effector locations without stressing the model or system hardware beyond tolerable values. We have not yet investigated the effect of varying the wire-length tolerance on execution time in the various test conditions.

Improvements to the current statics model may yield better results in future trials. The statics model currently uses several linear approximations to determine the directions of the tensions applied to the end-effector. While it is possible that the ellipsoid surface may only marginally affect the tension vectors relative to current estimates, future work must be done to validate these assumptions. Parameters in the statics model such as the desired normal force applied to the surface of the heart are currently set using general intuition. As these parameters may affect the efficiency and movement of the Cerberus system, further testing and experiments should be done to optimize these values for safety in clinical use. Furthermore, while the current inverse geodesics and statics model solver work effectively for a prolate ellipsoid, their effectiveness on the more irregular curved surface of the heart with periodic deformations from beating is not yet known. Further work on the Cerberus platform is required to optimize the statics and inverse kinematics solutions for more realistic heart models. Additional future work will focus on hardware upgrades for more rapid execution.

References

[1] J.-S. Hulot, K. Ishikawa, and R. J. Hajjar, "Gene therapy for the treatment of heart failure: promise postponed," *European Heart Journal*, vol. 37, no. 21, pp. 1651–1658, 2016.

[2] C. Naim, A. Yerevanian, and R. J. Hajjar, "Gene therapy for heart failure: where do we stand?" *Current Cardiology Reports*, vol. 15, no. 2, p. 333, 2013.

[3] M. Hedman, J. Hartikainen, and S. Ylä-Herttuala, "Progress and prospects: hurdles to cardiovascular gene therapy clinical trials," *Gene Therapy*, vol. 18, no. 8, pp. 743–749, 2011.

[4] K. Ishikawa, L. Tilemann, K. Fish, and R. J. Hajjar, "Gene delivery methods in cardiac gene therapy," *Journal of Gene Medicine*, vol. 13, no. 10, pp. 566–572, 2011.

[5] B. Ritwick, K. Chaudhuri, G. Crouch, J. R. M. Edwards, M. Worthington, and R. G. Stuklis, "Minimally invasive mitral valve procedures: the current state," *Minimally Invasive Surgery*, vol. 2013, p. 679276, 2013.

[6] R. Brewer, P. F. Theurer, C. M. Cogan, G. F. Bell, R. L. Prager, G. Paone, *et al.*, "Morbidity but not mortality is decreased after off-pump coronary artery bypass surgery," *Annals of Thoracic Surgery*, vol. 97, no. 3, pp. 831–836, 2014.

[7] T. Ota, N. A. Patronik, D. Schwartzman, C. N. Riviere, and M. A. Zenati, "Minimally invasive epicardial injections using a novel semi-autonomous robotic device," *Circulation*, vol. 118, no. 14 suppl 1, pp. S115–S120, 2008.

[8] A. D. Costanza, M. S. Breault, N. A. Wood, M. J. Passineau, R. J. Moraca, and C. N. Riviere, "Parallel force/position control of an epicardial parallel wire robot," *IEEE Robotics and Automation Letters*, vol. 1, no. 2, pp. 1186–1191, 2016.

[9] A. Trevisani, P. Gallina, and R. L. Williams, "Cable-direct-driven robot (CDDR) with passive scara support: theory and simulation," *Journal of Intelligent and Robotic Systems*, vol. 46, no. 1, pp. 73–94, 2006.

[10] N. A. Wood, D. Schwartzman, M. A. Zenati, and C. N. Riviere, "Physiological motion modeling for organ-mounted robots," *International Journal of Medical Robotics and Computer Assisted Surgery*, vol. 13, no. 4, p. e1805, 2017.

[11] P. H. Borgstrom, B. L. Jordan, B. J. Borgstrom, M. J. Stealey, G. S. Sukhatme, M. A. Batalin, and W. J. Kaiser, "Nims-pl: A cable-driven robot with self-calibration capabilities," *IEEE Transactions on Robotics*, vol. 25, no. 5, pp. 1005–1015, 2009.

[12] R. L. Williams II and P. Gallina, "Translational planar cable-direct-driven robots," *Journal of Intelligent and Robotic Systems*, vol. 37, pp. 69–96, 2003.

[13] A. D. Costanza, N. A. Wood, M. J. Passineau, R. J. Moraca, S. H. Bailey, T. Yoshizumi, and C. N. Riviere, "A parallel wire robot for epicardial interventions," in *Proc. Annu. Int. Conf. IEEE Engineering in Medicine and Biology Society*, 2014, pp. 6155–6158.

[14] C. F. F. Karney, "Algorithms for geodesics," *Journal of Geodesy*, vol. 87, no. 1, pp. 43–55, 2013.